

# Identification of Respiration Types Through Respiratory Signal Derived From Clinical and Wearable Electrocardiograms

Agnese Sbrollini , Member, IEEE, Micaela Morettini , Member, IEEE, Ennio Gambi , Senior Member, IEEE, and Laura Burattini , Member, IEEE

**Abstract—Goal:** To evaluate suitability of respiratory signals derived from clinical 12-lead electrocardiograms (ECGs) and wearable 1-lead ECG to identify different respiration types. **Methods:** ECGs were simultaneously acquired through the M12R ECG Holter by Global Instrumentation and the chest strap BioHarness 3.0 by Zephyr from 42 healthy subjects alternating normal breathing, breath holding, and deep breathing. Respiration signals were derived from the ECGs through the Segmented-Beat Modulation Method (SBMM)-based algorithm and the algorithms by Van Gent, Charlton, Soni and Sarkar, and characterized in terms of breathing rate and amplitude. Respiration classification was performed through a linear support vector machine and evaluated by F1 score. **Results:** Best F1 scores were 86.59%(lead V2) and 80.57%, when considering 12-lead and 1-lead ECGs, respectively, and using SBMM-based algorithm. **Conclusion:** ECG-derived respiratory signals allow reliable identification of different respiration types even when acquired through wearable sensors, if associated to appropriate processing algorithms, such as the SBMM-based algorithm.

**Index Terms—**Apnea, deep breathing, normal breathing, electrocardiogram-derived respiration, segmented-beat modulation method.

**Impact Statement—**The Segmented-Beat Modulation Method-based algorithm efficiently derives respiration signals from both clinical and wearable electrocardiograms, allowing reliable classification of respiration types.

## I. INTRODUCTION

**B**REATHING is a vital biological process, the characterization of which is a cornerstone in many clinical applications finalized to assess pathological conditions such as lung diseases, acute respiratory distress syndrome, and respiratory muscles diseases [1], [2]. Breathing can be evaluated by analyzing the

respiration signal, which represents the air volume that moves in or out of the lungs with time. The respiration signal is directly acquired by spirometry and its most important features are breathing rate (BR) and breathing amplitude (BA). BR is defined as the number of breaths per minute and, in healthy adults, its normal value ranges between 12 bpm and 20 bpm [2]. BA is the volume of air that moves in and out of the lungs with each respiratory cycle [1] and, in healthy adults, it ranges between 300 mL and 500 mL [1], [3]. Despite BR being considered as a primary index for breathing evaluation, information provided by BA is also essential [4], [5], [6]. Indeed, BR and BA reflect two different physiological mechanisms: BR is mainly regulated by the autonomic nervous system, while BA is specifically regulated by metabolic inputs [4], [6]; moreover, they present an unbalanced association, being BA continuously adjusted according to BR, but not vice versa [5], [7].

Continuous and reliable respiration monitoring is essential in clinics (e.g., intensive care units) [8] but also in other contexts strictly related to healthcare (e.g., in-home monitoring or exercise monitoring) [9]. Unfortunately, direct measurement of breathing through spirometry is still uncomfortable for the subject (Fig. 1A). Consequently, several alternative and indirect methodologies for acquiring the respiratory signal have been proposed to minimize the involvement of the patient and maximize comfort. Among these, a commonly used methodology is the respiratory signal derived from the electrocardiogram (ECG), thus called ECG-derived respiration (EDR) signal [10], [11], [12], [13]. The algorithms implementing this methodology rely on the measurement of the ECG variations induced by respiration, mainly baseline wanders, amplitude modulation and heart-rate modulation (the former also called respiratory sinus arrhythmia). Algorithms based on ECG baseline wanders and amplitude modulation typically provide BR and an indirect measure of BA in  $\mu V$  (as the ECG) whereas algorithms based on the heart-rate modulation provide BR and an indirect measure of BA in bpm (as the heart rate) [10], [11], [12], [13]. Since the above-mentioned ECG variations may be more evident in some ECG leads rather than in others, multi-lead ECG acquisitions are usually considered. Even though multi-lead electrocardiography is more comfortable than spirometry (Fig. 1B), the success and widespread diffusion of the EDR methodology for monitoring respiration will depend on the possibility of using wearable

Manuscript received 31 August 2023; revised 30 October 2023 and 1 December 2023; accepted 8 December 2023. Date of publication 15 December 2023; date of current version 29 December 2023. This work was supported by the Project Challenge under Grant CUP B39J2200305000. The review of this article was arranged by Editor Riccardo Barbieri. (Corresponding author: Laura Burattini.)

The authors are with the Department of Information Engineering, Università Politecnica delle Marche, 60121 Ancona, Italy (e-mail: a.sbrollini@staff.univpm.it; m.morettini@univpm.it; e.gambi@univpm.it; l.burattini@univpm.it).

Digital Object Identifier 10.1109/OJEMB.2023.3343557

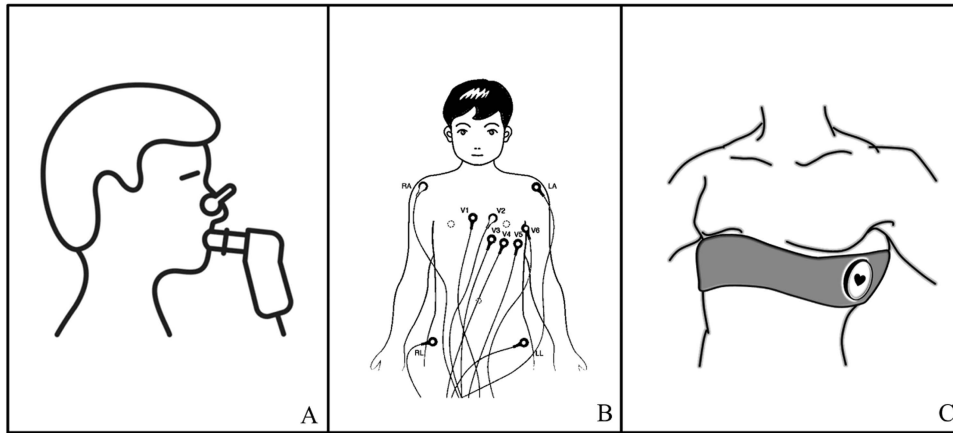


**Fig. 1.** Direct measurement of breathing through spirometry (panel A) and measurements of electrocardiogram through multi-lead electrocardiography (panel B) and wearable sensors (panel C) for the indirect measurement of the respiration signal.

**TABLE I**  
DEMOGRAPHIC AND HABITS DATA OF THE STUDY POPULATION

	Number	Age (yrs)	Height (cm)	Weight (kg)	Body mass Index (kg/m <sup>2</sup> )	Smoker (Yes/No)	Athlete (Yes/No)
<i>Male</i>	18	23[21;24]	180[178;182]	74[69;78]	22.9[21.7;24.0]	11/13	17/7
<i>Female</i>	24	22[21;23]	162[160;169]	56[53;61]	21.1[20.1;23.4]	6/18	8/16
<i>Overall</i>	42	22[21;23]	170[163;179]	64[56;72]	22.6[20.9;23.6]	23/29	29/23

sensors (such as bands or patches), which are extremely comfortable and subject-independent (Fig. 1C). Additionally, EDR success will depend on its suitability to discriminate among different types of respiration, such as normal breathing, breath holding (simulated apnea), and deep breathing. Thus, the double purpose of this work was: to acquire ECG data in controlled respiratory conditions including normal breathing, breath holding, and deep breathing; and to evaluate the suitability of respiratory signals derived from 12-lead ECGs obtained through an Holter ECG recorder and from 1-lead ECGs obtained through a wearable sensor, to characterize and discriminate the different respiration types.

## II. MATERIALS AND METHODS

### A. Electrocardiographic Data Acquisition

Data consisted of ECG signals simultaneously acquired through the clinical M12R Global Instrumentation Holter ECG recorder (<http://www.globalinstrumentation.com>) and the wearable chest-strap BioHarness 3.0 by Zephyr ([www.zephyranywhere.com](http://www.zephyranywhere.com)) from 42 healthy subjects (i.e., no known presence of cardiorespiratory diseases at the acquisition date) at the Cardiovascular Bioengineering Lab of the Università Politecnica delle Marche, Italy. Subjects' demographic data (sex, age, height, weight, and body mass index) and habits (smoker and athlete) are reported in Table I. The M12R Holter ECG recorder provided standard 12-lead (I; II; III; aVR; aVL; aVF; V1; V2; V3; V4; V5; V6) ECGs [14], [15] by considering the Mason-Likar electrodes configuration [16], with a sampling frequency of 1000 Hz and an amplitude resolution of 1  $\mu$ V. The

chest-strap BioHarness 3.0 provided 1-lead ECGs [17], [18] by positioning the sensor under the left arm (as suggested in the user's manual), with a sampling frequency of 250 Hz and an amplitude resolution of 1  $\mu$ V. All subjects gave their informed consent prior to data collection and acquisitions, which were undertaken in compliance with ethical principles of the Helsinki Declaration and approved by the institutional expert committee. During the ECG acquisitions, each subject was asked to follow a protocol that included a 5-fold repetition of the following respiratory sequence: 1 minute of normal breathing (NB), 30 s of autonomous breath holding (BH, simulated apnea), 1 minute of NB, and one deep breath (DB). Thus, a total of ten 1-minute normal breathing phases, five 30-second breath-holding phases, and 5 deep breaths were considered for each subject.

Data can be obtained by directly contacting the corresponding author (Laura Burattini, [l.burattini@univpm.it](mailto:l.burattini@univpm.it)).

### B. Electrocardiographic Data Pre-Processing

Each ECG recording was split into 30-second windows; only the first 5 NB windows, the 5 BH windows, and the 5 DB windows were considered for further processing. All ECG windows (independently from the acquisition device) were resampled to 200 Hz, filtered with a bidirectional 6th-order low-pass Butterworth filter with 40 Hz cut-off frequency, and processed with the ECGdeli algorithm [19] for R-peak detection.

### C. Electrocardiogram-Derived Respiration Signals

*EDR signal by SBMM-based algorithm:* Preprocessed ECG windows and their R-peak positions were submitted to the

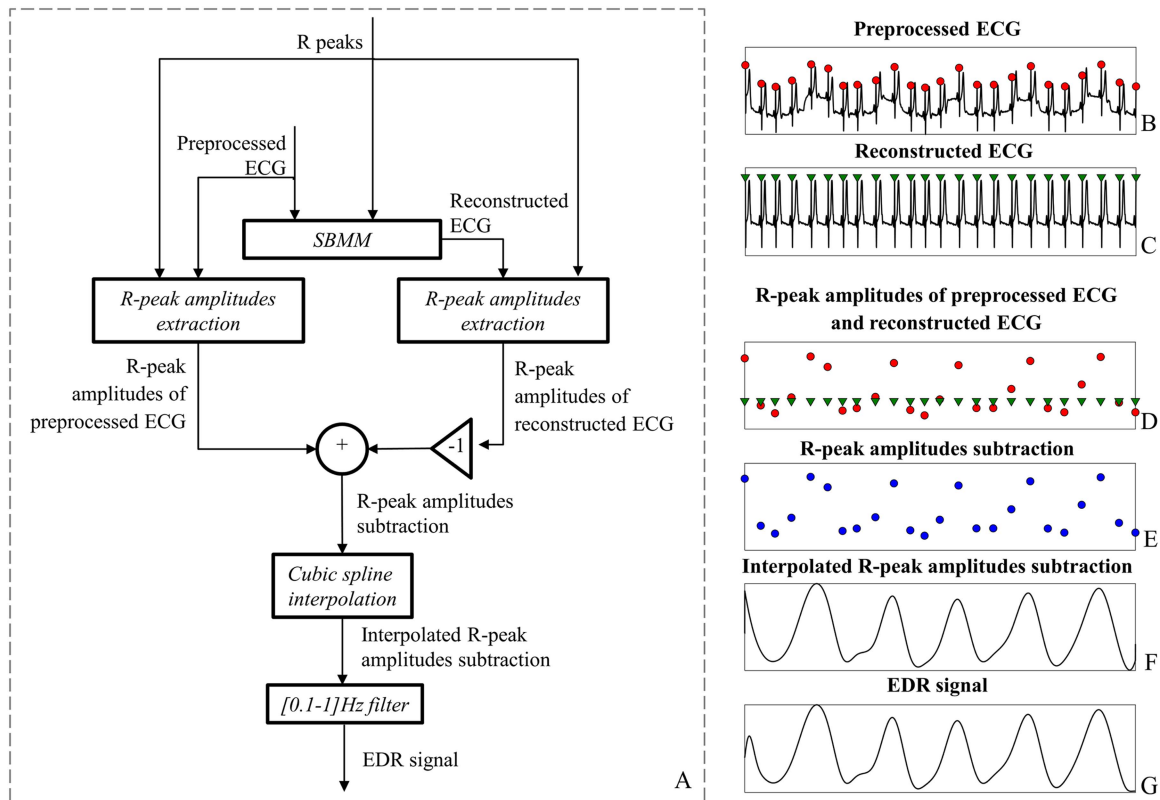


**Fig. 2.** Block diagram (panel A) of the segmented-beat modulation method (SBMM)-based algorithm to get for the electrocardiogram (ECG)-derived respiration (EDR) signal, together with an illustrative example: preprocessed ECG (panel B), reconstructed ECG (panel C), R-peak amplitudes of preprocessed ECG and reconstructed ECG in red and green, respectively (panel D); R-peak amplitudes subtraction (panel E), interpolated R-peak amplitudes subtraction (panel F) and, EDR signal (panel G).

Segmented-Beat Modulation Method (SBMM)-based algorithm [18], [20], [21] for respiratory signal extraction. Block diagram of the SBMM-based algorithm is depicted in Fig. 2. Briefly, SBMM (Fig. 2A) segments each cardiac cycle (CC) in the preprocessed ECG (Fig. 2B) into a QRS segment, with constant length, and a TUP segment, the length of which depends on previous RR interval. Then, a CC template is constructed as the median CC, after TUP-segment modulation (stretching/compression) to have all CCs of the same length. Successively, the ECG is reconstructed (Fig. 2C) by template concatenation, after TUP-segment demodulation (compression/stretching) to get back the initial ECG length. By construction, reconstructed ECG is no longer affected by respiration modulation (Fig. 2C). Amplitudes of the R-peak identified on the preprocessed ECG and reconstructed ECG (Fig. 2D) are subtracted (Fig. 2E), interpolated using a cubic spline (Fig. 2F) and, eventually, filtered with a bidirectional 6th-order low-pass Butterworth filter with 1 Hz cut-off frequency to obtain the EDR signal (Fig. 2G).

The above described SBMM-based algorithm was implemented in MATLAB (R2022b).

*EDR signal by other methods:* The following algorithms by Van Gent et al. (VGE) [12], Charlton et al. (CHA) [13], Soni et al. (SON) [10] and Sarkar et al. (SAR) [11] were also considered. These four algorithms analyze the ECG to construct the heart-rate series, which is then filtered to get the EDR signal.

Specifically, VGE applies a 2nd-order band-pass Butterworth filter with 0.1 Hz and 0.4 Hz cut-off frequencies; CHA applies a 6th-order band-pass Butterworth filter with 0.06 Hz and 1 Hz cut-off frequencies; SON applies a 6th-order low-pass Butterworth filter with 0.5 Hz cut-off frequency; and SAR applies a 6th-order band-pass Butterworth filter with 0.1 Hz and 0.7 Hz cut-off frequencies.

All algorithms are implemented in the Python and available in the NeuroKit toolbox [22].

#### D. Respiratory Feature Extraction and Statistics

EDR signals were characterized in terms of BR (computed as median number of signal maxima and minima per minute) and BA (computed as median value of signal maxima minus minima). Normality of feature distribution was assessed by Lilliefors' test. Not-normal distribution were reported in terms of 50th (median)[25th;75th] percentiles. Comparison among BR and BA distributions corresponding to different respiration type was performed by the Wilcoxon ranksum test for equal medians.

To evaluate the ability of BR and BA in identifying occurrence of normal breathing, breath holding, and deep breathing, BR and BA were used to feed a linear support vector machine (SVM) for NB, BH, and DB classification. Classification performance was evaluated by computing the F1 score from the confusion

**TABLE II**  
FEATURE DISTRIBUTION OF EDR EXTRACTED BY SBMM-BASED ALGORITHM, VGE, CHA, SON AND SAR FROM 12-LEAD ECG AND 1-LEAD ECG REPORTED IN TERMS OF 50TH (MEDIAN)[25TH;75TH] PERCENTILES

Respiration			12-lead ECG											1-lead ECG		
Feature	Type	I	II	III	aVR	aVL	aVF	V1	V2	V3	V4	V5	V6			
SBMM-based algorithm	BR (cpm)	NB	10*[3;15]	4*[3;13]	7*[3;13]	6*[3;13]	10*[3;15]	4*[3;13]	13*[10;18]	15*[10;18]	10*[3;15]	13*[6;16]	12*[3;15]	12*[4;15]	15*[10;18]	
		BH	3*[1;4]	3*[1;4]	3*[1;4]	3*[1;4]	3*[1;4]	3*[1;4]	3*[1;4]	3*[1;4]	3*[1;4]	1*[1;3]	1*[1;3]	3*[1;4]	3*[1;6]	
		DB	4*[3;7]	4*[3;6]	3[3;6]	4[3;6]	4[3;7]	4*[3;6]	6[3;9]	4*[3;9]	4[3;7]	3[3;6]	3[3;6]	3[3;6]	6[3;12]	
	BA (μV)	NB	174*	541*	563*	314*	317*	536*	424*	607*	285*	446*	448*	436*	202*	
		BH	[121;256]	[387;829]	[389;841]	[217;452]	[209;527]	[396;875]	[307;592]	[389;883]	[188;457]	[284;668]	[312;766]	[273;678]	[138;309]	
		DB	179*	564*	606*	313*	358*	559*	387*	445*	277*	483*	498*	367*	219*	
	VGE algorithm	BR (cpm)	NB	12*[9;13]	12*[10;15]	12*[9;15]	12*[9;15]	12*[10;15]	12*[9;15]	12*[10;15]	12*[9;15]	12*[9;15]	12*[9;15]	12*[9;15]	12*[9;15]	12*[9;15]
			BH	9*[7;10]	9*[7;10]	9*[7;10]	9*[7;10]	9*[7;10]	9*[7;10]	9*[7;10]	9*[7;10]	9*[7;10]	9*[7;10]	9*[7;10]	9*[7;10]	9*[7;10]
			DB	9*[7;10]	9*[7;10]	9*[7;10]	9*[7;10]	9*[7;12]	9*[7;10]	9*[7;10]	9*[7;10]	9*[7;10]	9*[7;10]	9*[7;10]	9*[7;10]	9*[7;12]
BA (bpm)		NB	9[6;12]	8*[6;11]	8*[6;11]	9[6;12]	9[6;12]	8*[6;11]	8*[6;11]	8*[6;11]	8*[6;11]	8*[6;11]	8*[6;11]	8*[6;11]	8*[6;11]	
		BH	5*[3;7]	5*[3;6]	5*[3;6]	5*[3;7]	5*[3;7]	5*[3;6]	5*[3;6]	5*[3;6]	5*[3;6]	5*[3;6]	5*[3;6]	5*[3;6]	5*[3;7]	
		DB	12*[9;16]	11*[8;15]	11*[8;15]	12*[9;15]	12*[9;16]	11*[8;15]	11*[9;15]	11*[8;15]	11*[8;15]	11*[8;15]	11*[8;15]	11*[8;15]	13*[9;18]	
CHA algorithm		BR (cpm)	NB	12*[7;15]	12*[7;15]	12*[7;15]	12*[9;15]	12*[9;15]	12*[7;15]	12*[9;15]	12*[7;15]	12*[7;15]	12*[7;13]	12*[7;15]	12*[7;13]	12*[7;15]
			BH	7*[6;9]	7*[6;9]	7*[6;9]	7*[6;9]	7*[6;9]	7*[6;9]	7*[6;9]	7*[6;9]	7*[6;9]	7*[6;9]	7*[6;9]	7*[6;9]	7*[6;9]
			DB	7*[6;9]	7*[6;9]	7*[6;9]	7*[6;9]	7*[6;9]	7*[6;9]	7*[6;9]	7*[6;9]	7*[6;9]	7*[6;9]	7*[6;9]	7*[6;9]	7*[6;10]
	BA (bpm)	NB	11[8;14]	10[7;13]	10[7;14]	11[8;15]	11*[8;14]	10[7;13]	10[7;13]	10[7;14]	10[7;14]	10[7;14]	10[7;13]	10[7;13]	10[7;14]	
		BH	8*[5;12]	7*[5;11]	7*[5;11]	8*[5;13]	8*[5;14]	7*[5;11]	7*[5;11]	7*[5;11]	7*[5;11]	7*[5;11]	7*[5;11]	7*[5;11]	8*[5;11]	
		DB	17*[11;22]	15*[11;19]	15*[11;19]	17*[12;22]	17*[12;23]	15*[11;19]	15*[11;19]	15*[11;19]	15*[11;19]	15*[11;19]	15*[11;19]	15*[11;19]	17*[12;24]	
	SON algorithm	BR (cpm)	NB	6*[1;12]	6*[1;12]	7*[1;12]	6*[1;12]	6*[3;12]	6*[1;12]	6*[1;12]	6*[1;12]	6*[1;12]	6*[1;12]	6*[1;12]	6*[1;12]	6*[1;12]
			BH	1*[1;3]	1*[1;3]	1*[1;3]	1*[1;3]	1*[1;3]	1*[1;3]	1*[1;3]	1*[1;3]	1*[1;3]	1*[1;3]	1*[1;3]	1*[1;3]	1*[1;3]
			DB	4*[3;7]	4*[3;7]	4*[4;7]	6*[4;7]	4*[3;7]	4*[3;7]	4*[3;7]	4*[3;7]	4*[3;7]	4*[3;7]	4*[3;7]	4*[3;7]	6*[4;7]
BA (bpm)		NB	15*[10;22]	14*[10;20]	14*[10;20]	15*[10;20]	15*[11;21]	14*[10;19]	14*[10;20]	14*[10;20]	14*[10;20]	14*[10;20]	14*[10;19]	14*[10;20]	15*[10;22]	
		BH	17*[11;24]	16[11;23]	16[11;23]	17[11;25]	17*[11;25]	16[11;23]	16[11;23]	16[11;23]	16[11;23]	16[11;23]	16[11;23]	16[11;23]	17*[11;24]	
		DB	22*[17;29]	20*[16;26]	20*[16;26]	20*[16;26]	22*[17;27]	20*[16;26]	20*[16;26]	20*[16;26]	21*[16;26]	21*[16;26]	21*[16;26]	20*[16;26]	23*[18;31]	
SAR algorithm		BR (cpm)	NB	12*[10;15]	12*[9;15]	12*[9;15]	13*[10;15]	12*[10;15]	12*[9;15]	12*[10;15]	12*[9;15]	12*[9;15]	12*[9;15]	12*[9;15]	12*[9;15]	12*[10;15]
			BH	9*[7;10]	9*[7;10]	9*[7;10]	9*[7;12]	9*[7;12]	9*[7;10]	9*[7;10]	9*[7;10]	9*[7;10]	9*[7;10]	9*[7;10]	9*[7;10]	9*[7;12]
			DB	9*[7;12]	9*[7;10]	9*[7;10]	9*[7;12]	9*[7;12]	9*[7;10]	9*[7;10]	9*[7;10]	9*[7;10]	9*[7;10]	9*[7;10]	9*[7;10]	9[9;13]
	BA (bpm)	NB	9*[6;13]	8*[6;12]	8*[6;12]	9*[7;13]	10*[8;13]	8*[6;12]	9*[6;12]	9*[6;12]	9*[7;12]	8*[6;12]	9*[6;12]	8*[6;12]	9*[6;12]	
		BH	5*[4;8]	5*[3;7]	5*[3;7]	5*[4;8]	6*[4;9]	5*[3;7]	5*[3;7]	5*[3;7]	5*[3;7]	5*[3;7]	5*[3;7]	5*[3;7]	5*[4;7]	
		DB	12*[9;17]	12*[9;15]	12*[9;15]	12*[10;16]	13*[10;17]	12*[9;15]	12*[9;16]	12*[9;15]	12*[9;15]	11*[9;15]	12*[9;15]	12*[9;15]	13*[9;18]	

\* P value lower than 0.05, when comparing the feature distribution of an event class vs. the jointed feature distribution of the other two classes. BA: breathing amplitude; BH: breath holding; BR: breathing rate; CHA: Charlton et al. [13] algorithm; DB: deep breathing; ECG: electrocardiogram; EDR: electrocardiogram-derived respiration; NB: normal breathing; SAR: Sarkar et al. [11] algorithm; SBMM: Segmented-Beat Modulation Method; SON: Soni et al. [10] algorithm; VGE: Van Gent et al. [12] algorithm.

matrix, computed as:

$$F1 = \frac{2 \cdot TC}{2 \cdot TC + MC} \quad (1)$$

where TC is the number of correct classifications and MC is the number of misclassifications. Moreover, SVM scores were used to compute the area under the curve (AUC) of the received operating characteristic. Statistical significance (P value) of all statistical analyses was set at 0.05.

### III. RESULTS

Distributions of BR and BA from EDR signals were found to be not normal and are reported in Table II. When using SBMM-based algorithm, significant differences were observed among BR distributions of all respiration types in 5 leads (I, II, aVF, V2, and V6) of 12-lead ECGs, and among BA distributions of all respiration types in all leads of 12-lead ECGs and in the 1-lead ECGs. Consequently, the most discriminating feature was BA and the most difficult respiration type to be discriminated was DB. When using VGE, significant differences were observed among BR distributions of all respiration types in all leads of 12-lead ECGs, and among BA distributions of

all respiration types in 9 leads (II, III, aVF, V1, V2, V3, V4, V5 and V6) of 12-lead ECGs and in the 1-lead ECGs. Consequently, the most discriminating feature was BR when analyzing the 12-lead ECGs, and BA when analyzing the 1-lead ECGs. The most difficult respiration type to be discriminated was NB when analyzing the 12-lead ECGs, and DB when analyzing the 1-lead ECGs. When using CHA, significant differences were observed among BR distributions of all respiration types in all leads of 12-lead ECGs, and among BA distributions of all respiration types in 2 leads (aVL and V2) of 12-lead ECGs and in the 1-lead ECG. Consequently, the most discriminating feature was BR when analyzing the 12-lead ECGs, and BA when analyzing the 1-lead ECGs. The most difficult respiration type to be discriminated was NB when analyzing the 12-lead ECGs, and DB when analyzing the 1-lead ECGs. When using SON, significant differences were observed among BR distributions of all respiration types in all leads of 12-lead ECGs and in the 1-lead ECG, and among BA distributions of all respiration types in 2 leads (I and aVL) of 12-lead ECG and in the 1-lead ECG. Consequently, the most discriminating feature was BR when analyzing the 12-lead ECGs. The most difficult respiration type to be discriminated was BH when analyzing the 12-lead

**TABLE III**  
F1 SCORE OF SVM CONSTRUCTED USING BREATHING RATE AND AMPLITUDE MEASURED IN EDR FROM 12-LEAD AND 1-LEAD ECGS

F1 score (%)	12-lead ECG												1-lead ECG
	I	II	III	aVR	aVL	aVF	V1	V2	V3	V4	V5	V6	
SBMM-based algorithm	72.34	70.24	73.62	72.21	76.95	70.64	84.08*	86.59* <sup>§</sup>	77.07	83.55*	82.02*	84.30*	80.57*
VGE algorithm	78.50	79.65	79.43	77.55	77.67	79.31	78.85	78.96	79.31	79.31	79.19	78.96	77.79
CHA algorithm	77.67	79.54	79.31	77.55	76.11	79.89*	79.08	78.85	79.08	79.08	79.19	78.96	78.38
SON algorithm	75.37	74.00	74.38	75.12	74.50	74.63	74.13	74.00	74.00	74.25	74.38	74.13	74.25
SAR algorithm	78.85*	79.66*	79.77*	77.91*	77.19*	79.77	79.43	79.54	79.43*	79.89	78.96	79.31	77.55

\*: the highest F1 score among the 5 algorithms in each ECG lead. <sup>§</sup>: the highest F1 score among the five algorithms in all ECG leads. CHA: Charlton et al. [13] algorithm; ECG: electrocardiogram; EDR: electrocardiogram-derived respiration; SAR: Sarkar et al. [11] algorithm; SBMM: Segmented-Beat Modulation Method; SON: Soni et al. [10] algorithm; SVM: support vector machine; VGE: Van Gent et al. [12] algorithm.

**TABLE IV**  
AUC (%) OF SVM CONSTRUCTED USING BREATHING RATE AND AMPLITUDE MEASURED IN EDR FROM 12-LEAD AND 1-LEAD ECGS

	Respiration type	12-lead ECG												1-lead ECG
		I	II	III	aVR	aVL	aVF	V1	V2	V3	V4	V5	V6	
SBMM-based algorithm	NB	62.86	56.51	61.15	58.26	67.96*	55.67	78.22* <sup>§</sup>	74.36*	64.59	71.47*	65.28	67.09*	67.66*
	BH	78.67	74.11	73.67	75.98	79.50	72.32	85.10	88.32*	82.15	88.59* <sup>§</sup>	84.99	85.86	85.08*
	DB	78.52	76.14	76.08	76.62	79.12	76.15	81.16	85.60*	81.87	89.86* <sup>§</sup>	86.66*	86.43*	82.42*
VGE algorithm	NB	63.48	64.26	63.47	62.85	60.96	63.53	63.61	62.77	64.27	63.92	62.91	63.78	61.55
	BH	85.18	87.99*	87.51	85.14*	84.00*	87.77*	87.85*	87.55	87.89*	87.51	87.01	87.29*	85.01
	DB	79.53	83.32*	83.07*	79.67*	79.36*	83.35*	82.52	82.76	82.88*	82.45	82.79	82.58	80.90
CHA algorithm	NB	67.48*	65.12	65.27	59.57	58.29	67.02*	65.46	66.72	65.64	65.73	65.03	64.36	61.30
	BH	81.81	84.26	83.92	78.54	76.24	84.52	84.06	83.33	83.66	83.64	83.70	83.57	84.48
	DB	78.78	82.30	82.03	77.55	77.45	82.40	81.95	81.01	81.75	81.68	82.36	82.03	79.83
SON algorithm	NB	65.09	65.48*	65.51*	65.38*	64.40	65.91	65.49	65.52	66.02*	65.38	65.48*	65.39	64.40
	BH	79.85	81.15	81.63	81.51	79.65	81.75	81.44	81.19	81.71	81.92	81.67	81.62	82.52
	DB	80.76*	79.77	80.02	78.95	78.73	79.72	79.88	79.81	79.99	80.08	80.18	79.60	80.50
SAR algorithm	NB	64.46	63.99	63.73	60.46	56.58	63.67	62.53	63.29	64.01	64.66	63.07	63.49	60.97
	BH	85.69*	87.26	87.24*	82.06	80.36	86.89	86.97	86.77	87.42	87.57	87.37*	87.11	84.66
	DB	78.79	82.34	82.80	78.45	77.53	82.52	82.55*	81.87	81.71	81.80	82.16	82.09	78.75

\*: the highest F1 among the five methods in each ECG lead and for each type of respiration. <sup>§</sup>: the highest F1 score among the five methods in all ECG leads for each type of respiration. AUC: area under the curve of the receiver operating characteristic; BH: breath holding; CHA: Charlton et al. [13] algorithm; DB: deep breath; ECG: electrocardiogram; EDR: electrocardiogram-derived respiration; NB: normal breathing; SAR: Sarkar et al. [11] algorithm; SBMM: Segmented-Beat Modulation Method; SON: Soni et al. [10] algorithm; SVM: support vector machine; VGE: Van Gent et al. [12] algorithm.

ECGs. Eventually, when using SAR, significant differences were observed among BR distributions of all respiration types in all leads of 12-lead ECGs, and among BA distributions of all respiration types in all leads of 12-lead ECGs and in the 1-lead ECG. Consequently, the most discriminating feature was BA when analyzing the 1-lead ECGs. The most difficult respiration type to be discriminated was DB when analyzing the 1-lead ECGs.

Values of F1 score of SVM constructed by using BR and BA measured in the 12-lead ECGs and 1-lead ECGs are reported in Table III. When considering EDR signals from 12-lead ECGs, the highest F1 score among the 5 algorithms was obtained when using SON in leads I (78.85%), II (79.66%), III (79.77%), aVR (77.91%), aVL (77.19%) and V3 (79.43%), when using SBMM-based algorithm in leads V1 (84.08%), V2 (86.59%), V4

(83.55%), V5 (82.02%) and V6 (84.30%), and when using CHA in lead aVF (79.89%); thus, the overall highest F1 score over all 12-leads was obtained when using SBMM-based algorithm in V2 (86.59%). When considering EDR signals from 1-lead ECGs, the highest F1 score among the 5 algorithms was obtained when using SBMM-based algorithm (80.57%).

Values of AUC of constructed by using BR and BA measured in the 12-lead ECGs and 1-lead ECGs are reported in Table IV. When using SBMM-based algorithm, AUC values for NB, BH, and DB ranged from 55.67% (aVF) to 78.22% (V1), from 72.32% (aVF) to 88.59% (V4), and from 76.08% (III) to 89.86% (V4), respectively, over the leads of the 12-lead ECGs; instead, they were equal to 66.66%, 85.08% and 84.42% for the 1-lead ECGs. When using VGE, AUC values for NB, BH, and DB ranged from 60.96% (aVL) to 64.27% (V3), from 84.00% (aVL)

to 87.99% (II), and from 79.53% (I) to 83.32% (II), respectively, over the leads of the 12-lead ECGs; instead, they were equal to 61.55%, 85.01% and 80.90% for the 1-lead ECGs. When using CHA, AUC values for NB, BH, and DB ranged from 58.29% (aVL) to 67.48% (I), from 76.24% (aVL) to 84.52% (aVF), and from 77.45% (aVL) to 82.40% (aVF), respectively, over the leads of the 12-lead ECGs; instead, they were equal to 61.30%, 84.48% and 79.83% for the 1-lead ECGs. When using SON, AUC values for NB, BH, and DB ranged from 64.40% (aVL) to 66.02% (V3), from 79.65% (aVL) to 81.92% (V4), and from 78.73% (aVL) to 80.76% (V1), respectively, over the leads of the 12-lead ECGs; instead, they were equal to 64.40%, 82.52% and 80.50% for the 1-lead ECGs. Eventually, when using SAR, AUC values for NB, BH, and DB ranged from 56.58% (aVL) to 64.66% (V4), from 80.36% (aVL) to 87.57% (V4), and from 77.53% (aVL) to 82.80% (III), respectively, over the leads of the 12-lead ECGs; instead, they were equal to 63.07%, 87.37% and 82.16% for the 1-lead ECGs. Generally, for all algorithms, the most difficult respiration type to be correctly classified was NB and the easiest one was BH.

#### IV. DISCUSSION

In this work, ECG data was acquired in controlled respiratory conditions including normal breathing, breath holding (simulated apnea), and deep breathing to evaluate the suitability of ECG-derived respiratory signals to characterize and classify the different respiration types. Two kinds of ECG recorders were used, the clinical M12R (12 leads) Global Instrumentation Holter ECG machine and the wearable BioHarness 3.0 by Zephyr (1 lead), in order to investigate the possibility of using more and more comfortable devices with respect to spirometry. Comfortable and subject-independent devices, indeed, are particularly desirable in several monitoring settings [18]. The possibility to track the respiration features by using an ECG recording opens the possibility to continuously monitor the respiration every time that an ECG is acquired. For example, the standard device for cardiac monitoring, such as the cardiac Holter, may be used for respiration monitoring and, thus, to evaluate the respiratory stress of the patients in every moment of the daily life activity.

Acquired electrocardiograms were processed using five different algorithms: our Segmented-Beat Modulation Method-based algorithm [20], [21], based on respiration-related ECG amplitude modulation, and the open source [22] algorithms by Van Gent et al. [12], Charlton et al. [13], Soni et al. [10] and Sarkar et al. [11], based on respiration-related heart-rate modulation. Indirect electrocardiogram-derived respiratory signals were then characterized in terms of breathing rate and amplitude. Breathing features of the 630 signal segments (210 for each respiration type) were used to feed a linear support vector machine for classification of respiration types; this number is sufficient for evaluating the power of breathing features in discriminating respiration types (164 was the minimum number of samples for each respiration type with a power of the test equal to 80%). F1 score was used to evaluate overall multiclass classification performance, whereas the area under the curve of the receiver operating characteristic was used to evaluate the performance in identifying a specific respiration type.

When considering 12-lead ECGs, both performance indexes were higher in the precordial leads, and the best results were obtained when using the Segmented Beat Modulation Method (Tables III and IV). Thus, the precordial leads should be considered preferable for respiratory evaluations, possibly due to their location on the thorax that makes them very affected by amplitude modulation. Specifically, V2 seems to have the highest overall discrimination power (highest F1; Table III) while V4 seems to have the highest power to discriminate specific respiration types (highest area under the curve; Table IV). Similar results were obtained when considering 1-lead ECGs from the BioHarness 3.0, suggesting that simple single-lead wearable ECG sensors may be used to monitor respiration, especially if located on the thorax and if associated with appropriate processing algorithms. It could be argued that some wearable devices (such as the BioHarness 3.0 itself) integrate specific respiration sensors and provide respiration signals that likely allow more accurate evaluations than the respiration signals derived from the ECG (for example, application of the linear support vector machine to breathing rate and amplitude measured on the respiration signal provided by the BioHarness 3.0 provided excellent F1 score of 91.75%, and good area-under-the-curve values of 79.81%, 92.39%, and 97.04% for normal breathing, breath holding and deep breathing, respectively). Still, in long-lasting monitoring applications or in case of monitoring of small and fragile subjects (e.g., premature newborns), it may be important to reduce as much as possible hardware complexity of wearable devices, making simple sensors that record few signals from which to derive information of different physiological systems preferable.

The better performance of the Segmented-Beat Modulation Method-based algorithm over the other algorithms is due to the fact that it relies on ECG amplitude modulation rather than of heart-rate modulation. EDR methods based on amplitude modulation depend on electrode position and are able to better identify differences between extracted EDR. Consequently, the Segmented-Beat Modulation Method-based algorithm, possibly like other algorithms relying on ECG amplitude modulation [23], [24], provides a better estimation of breathing amplitude (Table II), which plays an important role in the identification of the breathing type [4], [5], [6]. This also explains why breath holding and deep breathing, which are the respiration types with the lowest and highest breathing amplitude, respectively, are better identified than normal breathing, which is the respiration type with the intermediate breathing amplitude.

Despite the promising results, this work is not free of limitations. The ECG measurements were done in a healthy population under laboratory conditions. This experimental setting was chosen because this work aimed to evaluate the best 12-lead ECG for the EDR estimation since, in real scenarios and available open-access datasets, the ECG measurements in pathological populations are usually performed with a reduced number of leads [25]. Moreover, this study considered phases of breath-holding that are different from real pathological apnea [26]. In the case of breath holding, the respiration is silent if measured by spirometry (no exchange of air), but a residual movement of the chest is easily visible if the respiration is measured by a chest strap on the rib cage [27]. This residual movement is a kind of noise that can jeopardize the correct interpretation of respiration

signals acquired by wearable sensors. This effect is also visible in our analysis; indeed, breathing rate and amplitude are not equal to zero in the breath-holding phases. Finally, considering the impossibility of simultaneously acquiring breathing by spirometry, this study could not support the evaluation of the association between breathing amplitude and tidal volume, important for a proper indirect estimation of tidal volume (in mL) [5]; and the identification of the best method in terms of breathing feature characterization, knowing that breathing features may depend on used signal processing procedures [28]. Future studies will aim to evaluate the performance of our method in a real pathological scenario, by considering real cases of apnea (no breath-holding events) and by comparing the results with data simultaneously acquired by spirometry.

## V. CONCLUSION

Respiration signals derived from electrocardiograms allow reliable identification of normal breathing, breath holding (simulated apnea), and deep breathing, even when acquired through wearable sensors, if these are located on the thorax and associated to appropriate processing algorithms such as the Segmented-Beat Modulation Method-based algorithm.

*Conflicts of Interest:* All authors declare no conflicts of interest.

*Author Contributions:* The authors confirm their contribution to the paper as follows: Conceptualization, A. Sbröllini and L. Burattini; methodology, A. Sbröllini and L. Burattini; software, A. Sbröllini; validation, A. Sbröllini, M. Morettini, E. Gambi and L. Burattini; formal analysis, A. Sbröllini, M. Morettini and L. Burattini; investigation, A. Sbröllini and M. Morettini; resources, L. Burattini; data curation, A. Sbröllini; writing—original draft preparation, A. Sbröllini; writing—review and editing, A. Sbröllini, M. Morettini, E. Gambi and L. Burattini; visualization, A. Sbröllini; supervision, L. Burattini; project administration, L. Burattini; funding acquisition, M. Morettini, E. Gambi and L. Burattini. All authors have read and agreed to the published version of the manuscript.

## REFERENCES

- [1] J. Hallett and F. Toro, "Physiology, tidal volume," in *StatPearls*, St. Petersburg, FL, USA: StatPearls Publishing, 2021. [Online]. Available: <https://www.ncbi.nlm.nih.gov/books/NBK482502/>
- [2] A. Nicolò, C. Massaroni, E. Schena, and M. Sacchetti, "The importance of respiratory rate monitoring: From healthcare to sport and exercise," *Sensors*, vol. 20, no. 21, Nov. 2020, Art. no. 6396.
- [3] R. Pierce, "Spirometry: An essential clinical measurement," *Australian Fam. Physician*, vol. 34, no. 7, pp. 535–539, Jul. 2005.
- [4] A. Nicolò, S. M. Marcora, I. Bazzucchi, and M. Sacchetti, "Differential control of respiratory frequency and tidal volume during high-intensity interval training," *Exp. Physiol.*, vol. 102, no. 8, pp. 934–949, Aug. 2017.
- [5] A. Sbröllini et al., "Estimation of tidal volume during exercise stress test from wearable-device measures of heart rate and breathing rate," *Appl. Sci.*, vol. 12, no. 11, May 2022, Art. no. 5441.
- [6] A. Nicolò, M. Girardi, and M. Sacchetti, "Control of the depth and rate of breathing: Metabolic vs. non-metabolic inputs," *J. Physiol.*, vol. 595, no. 19, pp. 6363–6364, Oct. 2017.
- [7] A. Nicolò, M. Girardi, I. Bazzucchi, F. Felici, and M. Sacchetti, "Respiratory frequency and tidal volume during exercise: Differential control and unbalanced interdependence," *Physiol. Rep.*, vol. 6, no. 21, Nov. 2018, Art. no. e13908.
- [8] J. J. Osborn, "Cardiopulmonary monitoring in the respiratory intensive care unit," *Med. Instrum.*, vol. 11, no. 5, pp. 278–282, 1977.
- [9] R. F. Alvarez, G. R. Cuadrado, F. R. Jerez, A. G. García, P. R. Menendez, and P. C. Clara, "Home mechanical ventilation through mask: Monitoring leakage and nocturnal oxygenation at home," *Respiration*, vol. 85, no. 2, pp. 132–136, 2013.
- [10] R. Soni and M. Muniyandi, "Breath rate variability: A novel measure to study the meditation effects," *Int. J. Yoga*, vol. 12, no. 1, 2019, Art. no. 45.
- [11] S. Sarkar, S. Bhattacharjee, and S. Pal, "Extraction of respiration signal from ECG for respiratory rate estimation," in *Proc. Michael Faraday Int. Eng. Technol. Int. Summit*, 2015, pp. 336–340.
- [12] P. van Gent, H. Farah, N. van Nes, and B. van Arem, "HeartPy: A novel heart rate algorithm for the analysis of noisy signals," *Transp. Res. Part F: Traffic Psychol. Behav.*, vol. 66, pp. 368–378, Oct. 2019.
- [13] P. H. Charlton, T. Bonnici, L. Tarassenko, D. A. Clifton, R. Beale, and P. J. Watkinson, "An assessment of algorithms to estimate respiratory rate from the electrocardiogram and photoplethysmogram," *Physiol. Meas.*, vol. 37, no. 4, pp. 610–626, Apr. 2016.
- [14] P. Pierleoni et al., "Simultaneously acquired data from contactless and wearable devices for direct and indirect heart-rate measurement," *Data Brief*, vol. 26, 2019, Art. no. 104436.
- [15] E. Gambi et al., "Heart rate detection using microsoft kinect: Validation and comparison to wearable devices," *Sensors*, vol. 17, no. 8, 2017, Art. no. 1776.
- [16] M. Sejersten et al., "Comparison of EASI-derived 12-lead electrocardiograms versus paramedic-acquired 12-lead electrocardiograms using mason-likar limb lead configuration in patients with chest pain," *J. Electrocardiol.*, vol. 39, no. 1, pp. 13–21, Jan. 2006.
- [17] A. Sbröllini et al., "Sport database: Cardiorespiratory data acquired through wearable sensors while practicing sports," *Data Brief*, vol. 27, Dec. 2019, Art. no. 104793.
- [18] A. Sbröllini et al., "Segmented-beat modulation method-based procedure for extraction of electrocardiogram-derived respiration from data acquired by wearable sensors during high-altitude activity," in *Proc. Comput. Cardiol.*, 2022, vol. 498, pp. 1–4.
- [19] N. Pilia, C. Nagel, G. Lenis, S. Becker, O. Dössel, and A. Loewe, "ECGdeli - an open source ECG delineation toolbox for MATLAB," *SoftwareX*, vol. 13, Jan. 2021, Art. no. 100639.
- [20] A. Sbröllini, I. Marcantoni, A. Nasim, M. Morettini, and L. Burattini, "Electrocardiogram-derived respiratory signal in sleep apnea by segmented beat modulation method," in *Proc. IEEE 23rd Int. Symp. Consum. Technol.*, 2019, pp. 279–282.
- [21] B. Pambianco, A. Sbröllini, I. Marcantoni, M. Morettini, S. Fioretti, and L. Burattini, "Electrocardiogram derived respiratory signal through the segmented-beat modulation method," in *Proc. IEEE 40th Annu. Int. Conf. Eng. Med. Biol. Soc.*, 2018, pp. 5681–5684.
- [22] D. Makowski et al., "NeuroKit2: A Python toolbox for neurophysiological signal processing," *Behav. Res. Methods*, vol. 53, no. 4, pp. 1689–1696, Aug. 2021.
- [23] S. Babaeizadeh, S. H. Zhou, S. D. Pittman, and D. P. White, "Electrocardiogram-derived respiration in screening of sleep-disordered breathing," *J. Electrocardiol.*, vol. 44, no. 6, pp. 700–706, Nov./Dec. 2011.
- [24] S. Tiinanen, K. Noponen, M. Tulppo, A. Kiviniemi, and T. Seppänen, "ECG-derived respiration methods: Adapted ICA and PCA," *Med. Eng. Phys.*, vol. 37, no. 5, pp. 512–517, May 2015.
- [25] M. M. van Gilst et al., "Protocol of the SOMNIA project: An observational study to create a neurophysiological database for advanced clinical sleep monitoring," *BMJ Open*, vol. 9, Nov. 2029, Art. no. e030996.
- [26] J. Xie et al., "The use of respiratory effort improves an ECG-based deep learning algorithm to assess sleep-disordered breathing," *Diagnostics*, vol. 13, no. 13, Jun. 2023, Art. no. 2146.
- [27] Z. Zhang et al., "Development of a respiratory inductive plethysmography module supporting multiple sensors for wearable systems," *Sensors*, vol. 12, pp. 13167–13184, Sep. 2012.
- [28] J. Leube et al., "Reconstruction of the respiratory signal through ECG and wrist accelerometer data," *Sci. Rep.*, vol. 3, no. 1, Sep. 2020, Art. no. 14530.

Open Access funding provided by 'Università Politecnica delle Marche' within the CRUI CARE Agreement